AIRHEAD: an *A*nthropomorph*I*c *R*ealistic *HEAD* phantom to test susceptibility artifact reduction techniques

K. Shmueli[1], P. Kinchesh[1], H. G. Parkes[1], D. L. Thomas[1], R. J. Ordidge[1]

[1]Wellcome Trust High Field MR Research Laboratory, Department of Medical Physics and Bioengineering, University College London, London, United Kingdom

Introduction: Susceptibility artifacts such as geometric distortion and drop-out are worse at high field strengths and are especially problematic in the T_2*-weighted rapid imaging sequences commonly used for BOLD contrast fMRI. A plethora of different susceptibility artifact reduction methods [**1,2,3**] have been proposed and it is important to systematically compare these to establish the optimum procedure for each brain region and purpose. Past investigations of MRI distortion have used simple phantoms such as arrangements of water-and air- filled spheres or cylinders [**4,5,6**] whose behaviour can be predicted using theory but the results can be difficult to relate to the real head.

Here the aim was to design and build a highly anthropomorphic head phantom to reproduce as accurately as possible the magnetic environment of the brain and provide a realistic and stable test object that, unlike human volunteers, can be scanned reproducibly, repeatedly and indefinitely. For the phantom to allow quantitation of susceptibility artifacts the optimum image will ideally be uniform in the brain cavity and zero elsewhere. It is well established [**7**] that the main (B_0) field variation is primarily due to the geometrical configurations of tissue and air compartments so these need to be included in the phantom, which should also have realistic magnetic susceptibilities.

Choice of Materials: The phantom was based around a plastic skull (Anatomical Chart Company) to ensure realistic brain dimensions. Susceptibilities of several candidate materials to simulate bone and soft tissues, including the plastic skull, were measured using a SQUID magnetometer (Quantum Design MPM-7). Samples of rat cortex and lamb bone were also measured as references for soft tissue and bone. The measured mass susceptibilities shown in **Figure 1** informed the choice of materials for the phantom. For example wax has the most suitable susceptibility to mimic soft tissue and generates no MR signal and the plastic skull susceptibility is similar to that of real bone.

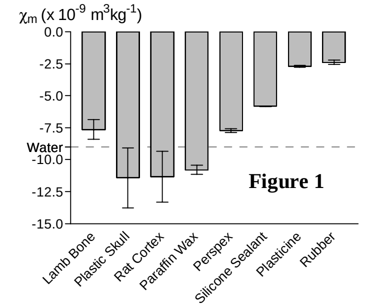

Figure 1

Phantom Construction and Filling: The plastic skull (**Fig 2C**) cavity was plugged with a large rubber bung (**Fig 2F**) and waterproofed using silicone sealant before filling with $MnCl_2$-doped water (**Fig 2D**). A $MnCl_2$ concentration of 0.1mM was chosen based on T_2 measurements of several $MnCl_2$ concentrations at 4.7T to try to simulate a mean T_2 of grey and white matter at 3-4.7T [**8,9,10**]. It is important to simulate T_2 since it determines T_2* and T_2*-weighted sequences suffer most from susceptibility artifacts. NaCl (31mM) was added to ensure that the phantom would load the RF coil.
An air bubble (**Fig 2B**) was left when filling to simulate the frontal sinus with the phantom supine.
Existing air spaces in the skull (nasal cavity and maxillary sinuses **Fig 2A**) were encased and additional ones were attached. For example the oral space was simulated by half a ping pong ball, the nasopharynx by two lengths of silicone rubber tubing and the auditory canals and mastoid air cells by two sealed lengths of the same tubing (**Fig 2E**). The dimensions of these air spaces were chosen to match real ones as closely as possible based on measurements made on a variety of MR and CT head images. A plastic (PETG) head-shaped mould (**Fig 2G**) was made and the filled skull plus air spaces was positioned inside it using rubber spacers before filling with molten wax (**Fig 2H**) to mimic soft tissues outside the brain.

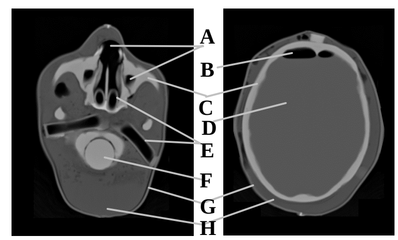

Figure 2: Transverse CT Images of the Phantom

Phantom Evaluation: The phantom was CT scanned to verify the position of the air spaces (see **Figure 2**). The phantom T_1 and T_2 were measured using sets of inversion-recovery FSE images with varying TI and standard SE images with varying TE respectively giving $T_1 = 1116 \pm 49$ ms and $T_2 = 80.6 \pm 0.2$ ms (fit value ± S.D.). All experiments were carried out on a SMIS MR 5000 4.7T whole-body MR scanner provided by Philips Medical Systems. B_0 maps of the phantom and three healthy volunteers were acquired (five volunteer maps and two phantom maps). For each map two short-TE gradient echo acquisitions were used with $\Delta TE = 1515$ or $4545\mu s$. The maps were unwrapped using PRELUDE software [**11**] and the volunteer maps had the brains extracted using the BET tool [**11**]. **Figure 3** shows B_0 field maps (Hz) of both the phantom and a volunteer. The standard deviation of the field in the maps of the phantom was 51.0 and 51.6Hz compared with 41.0, 42.6, 47.5, 49.4 and 62.2 Hz in the volunteers.

Discussion and Conclusions: An anthropomorphic head phantom has been successfully designed and constructed using materials of appropriate magnetic susceptibility and air spaces of realistic dimensions. As well as having a similar range of field values, B_0 field maps of the phantom and the brains of volunteers show many similarities including a higher-field region above the nasal air spaces, a lower-field region behind the frontal sinuses and a similar field pattern near the auditory air spaces. There remain some differences between the phantom and volunteer field maps, for example there is a higher-field region in the phantom at the base of the brain (**Figure 3 Coronal**) above the large rubber bung due to the reduced susceptibility of rubber compared with wax. This bung could be replaced with wax in future versions of the phantom. Since it has a similar magnetic field pattern, the phantom suffers from similar susceptibility artifacts to real heads and will therefore be useful for evaluating and comparing different susceptibility artifact reduction techniques. The phantom could also be a useful tool to test CT-MRI coregistration in the presence of susceptibility artifacts since the water-filled brain cavity is both CT and MR visible.

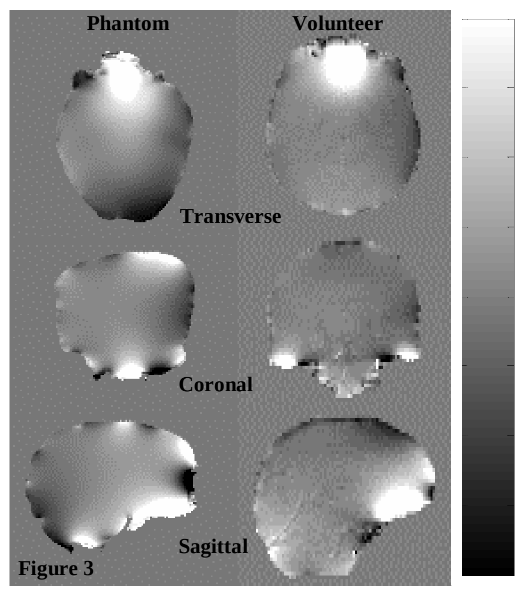

Figure 3

References:

1. R. Deichmann et al, Neuroimage 15:120-135 (2002)
2. V.A. Stenger et al, MRM 48:157-165 (2002)
3. J.L. Wilson et al, MRM 48:906-914 (2002)
4. A.M. Abduljalil et al, J. Comput. Assist. Tomogr. 23:832-841 (1999)
5. R.E. Drzymala, S. Mutic, Comput. Aided Surg. 4:248-255 (1999)
6. J-F. Daisne et al, Radiother. Oncol. 69 237-245 (2003)
7. S. Li et al, MRM 36:705-714 (1996)
8. J.P. Wansapura et al, JMRI 9:531-538 (1999)
9. P. Jezzard et al, Radiology 199:773-779 (1996)
10. Barfuss et al, Radiology 169:811-816 (1988)
11. www.fmrib.ox.ac.uk/fsl/

Acknowledgements: This work was supported by the Wellcome Trust. Thanks to Dr Q.Pankhurst, Dept. of Physics and Astronomy, University College London